Correction

IMMUNOLOGY AND INFLAMMATION

Correction for "TAp73 represses NF-κB–mediated recruitment of tumor-associated macrophages in breast cancer," by Johanna Wolfsberger, Habib A. M. Sakil, Leilei Zhou, Niek van Bree, Elena Baldisseri, Sabrina de Souza Ferreira, Veronica Zubillaga, Marina Stantic, Nicolas Fritz, Johan Hartman, Charlotte Rolny, and Margareta T. Wilhelm, which published March 1, 2021; 10.1073/pnas.2017089118 (*Proc. Natl. Acad. Sci. U.S.A.* **118**, e2017089118).

The authors note that Supporting Table S2 in the *SI Appendix* appeared incorrectly. Regarding this error, the authors note, "Sanger sequencing primers for the mouse and human Ccl2 gene have mistakenly been entered in the qPCR primer table (*SI Appendix*, Table S2) instead of the qPCR primer sequences for Ccl2 that were used in this study."

The authors also note that an error appeared in Fig. 3 and Fig. S3 in the *SI Appendix*. In both figures, the histograms are labeled DMSO but should instead be labeled siCtrl. The corrected figure and its legend appear below. The online version has been corrected, including the *SI Appendix* with the corrected Table S2 and Fig. S3.

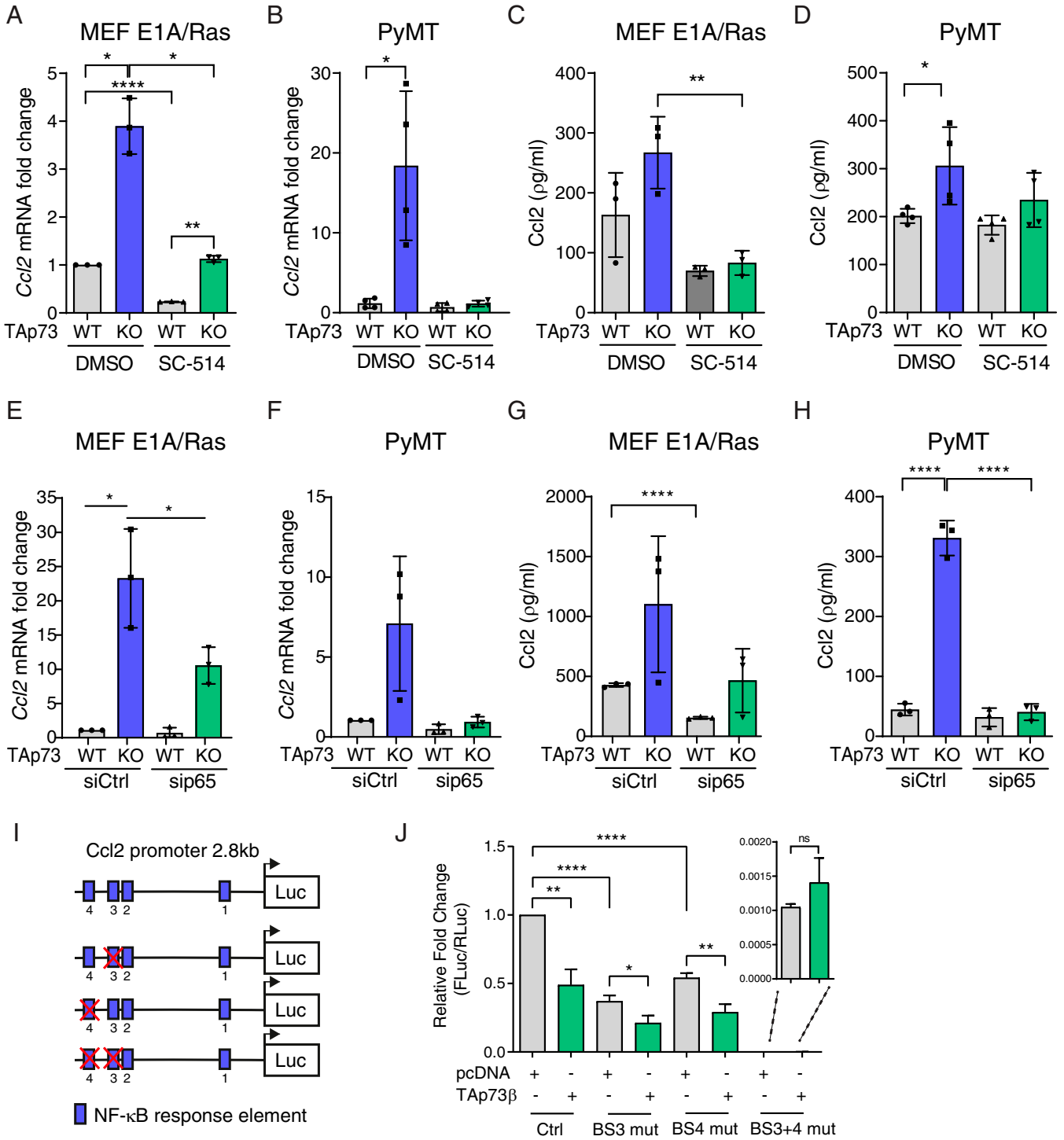

Fig. 3. TAp73 represses NF-κB–mediated regulation of Ccl2 expression. (*A*) qRT-PCR analysis of *Ccl2* mRNA levels in (*A*) TAp73 WT and KO MEF$^{E1A/Ras}$ ($n = 3$) and (*B*) PyMT/TAp73 WT or KO cells ($n = 4$) after 16-h treatment with NF-κB inhibitor SC-514 (100 μg/mL). ELISA analysis of Ccl2 protein secretion in conditioned media from (*C*) TAp73 WT and KO MEF$^{E1A/Ras}$ ($n = 3$) and (*D*) PyMT/TAp73 WT or KO cells ($n = 4$) after 16-h treatment with SC-514 (100 μg/mL). (*E* and *F*) qRT-PCR analysis of *Ccl2* mRNA levels in (*E*) TAp73 WT and KO MEF$^{E1A/Ras}$ ($n = 3$) and (*F*) PyMT/TAp73 WT or KO cells ($n = 3$) after 48-h treatment with sip65/RELA. (*G* and *H*) ELISA analysis of Ccl2 protein secretion in conditioned media from (*G*) TAp73 WT and KO MEF$^{E1A/Ras}$ ($n = 3$) and (*H*) PyMT/TAp73 WT or KO cells ($n = 3$) after 48-h treatment with sip65/RELA. (*I*) Schematics showing the murine Ccl2 promoter including NF-κB response elements, of which the distal BSs 3 and 4 were deleted either individually or simultaneously. (*J*) WT or mutated Ccl2 promoter luciferase reporter was cotransfected with TAp73β in HEK293 cells. Luciferase activity was measured 24 h after transfection and normalized to mock control ($n = 6$). All data are shown as mean ± SD $^*P < 0.05$, $^{**}P < 0.01$, $^{****}P < 0.0001$.

Published November 11, 2021.

www.pnas.org/cgi/doi/10.1073/pnas.2117333118

TAp73 represses NF-κB–mediated recruitment of tumor-associated macrophages in breast cancer

Johanna Wolfsberger[a], Habib A. M. Sakil[a], Leilei Zhou[a], Niek van Bree[a], Elena Baldisseri[a], Sabrina de Souza Ferreira[b], Veronica Zubillaga[a], Marina Stantic[a], Nicolas Fritz[a], Johan Hartman[c], Charlotte Rolny[b], and Margareta T. Wilhelm[a,1]

[a]Department of Microbiology, Tumor and Cell Biology, Karolinska Institutet, 171 65 Stockholm, Sweden; [b]Science for Life Laboratory, Department of Oncology–Pathology, Karolinska Institutet, Stockholm, 171 65, Sweden; and [c]Department of Oncology–Pathology, Karolinska Institutet, 171 64 Stockholm, Sweden

Edited by Tak W. Mak, University of Toronto, Toronto, ON, Canada, and approved January 5, 2021 (received for review August 13, 2020)

Infiltration of tumor-promoting immune cells is a strong driver of tumor progression. Especially the accumulation of macrophages in the tumor microenvironment is known to facilitate tumor growth and to correlate with poor prognosis in many tumor types. TAp73, a member of the p53/p63/p73 family, acts as a tumor suppressor and has been shown to suppress tumor angiogenesis. However, what role TAp73 has in regulating immune cell infiltration is unknown. Here, we report that low levels of TAp73 correlate with an increased NF-κB–regulated inflammatory signature in breast cancer. Furthermore, we show that loss of TAp73 results in NF-κB hyperactivation and secretion of Ccl2, a known NF-κB target and chemoattractant for monocytes and macrophages. Importantly, TAp73-deficient tumors display an increased accumulation of protumoral macrophages that express the mannose receptor (CD206) and scavenger receptor A (CD204) compared to controls. The relevance of TAp73 expression in human breast carcinoma was further accentuated by revealing that TAp73 expression correlates negatively with the accumulation of protumoral CD163$^+$ macrophages in breast cancer patient samples. Taken together, our findings suggest that TAp73 regulates macrophage accumulation and phenotype in breast cancer through inhibition of the NF-κB pathway.

p73 | NF-κB | tumor-associated macrophages | breast cancer

Inflammation plays an essential role in cancer development and progression and can promote both protumoral and anti-tumoral functions. Inflammation, in many cases, is elicited by the tumor itself and can be induced by several stimuli including cell death, hypoxia, oncogene activation, or loss of tumor-suppressor functions (1, 2). The nuclear factor kappa beta (NF-κB) pathway acts as a master regulator of inflammation and activation of NF-κB in cancer cells leads to secretion of cytokines and chemokines that attract immune cells to the tumor microenvironment (TME) (3–5). Macrophages are dominating the immune composition of most breast cancers and are plastic cells that can acquire a spectrum of tumor inhibitory phenotypes with the ability to restrict tumor growth and tumor cell spreading to secondary tumors (6). However, as tumors progress, the majority of tumor-associated macrophages (TAMs) acquire a protumoral phenotype that stimulates angiogenesis and facilitates tumor cell intravasation and metastatic dissemination (7–9). High macrophage infiltration has been found to correlate with poor patient survival in almost all solid cancers, including breast cancer (7, 10, 11). CCL2 is one of the key chemokines for monocyte recruitment to the tumor site, which will differentiate into macrophages that can acquire either a pro- or antitumoral phenotype. During tumor growth, CCL2 is highly expressed both at the tumor site and at the metastatic site, which leads to an extensive macrophage accumulation, promoting angiogenesis and metastasis. Consequently, its up-regulation has been associated with poor patient survival in breast cancer (12, 13).

The p73 gene, a member of the p53 family, encodes multiple isoforms with distinct biological functions. Alternative promoters give rise to either TAp73 isoforms, which have transactivation domains and act as transcription factors, or N-terminal truncated isoforms referred to as ΔNp73, which lack the transactivation domain and act as a dominant negative (14). In addition, alternative splicing in the C terminus allows for up to seven additional isoforms (α-η); TAp73α/β and ΔNp73α/β being most abundantly expressed (15). Unlike p53, the p73 gene is rarely mutated, and it is thought that a shift in the balance between TAp73 and ΔNp73 isoforms drives tumorigenesis. An increase of the ΔNp73 isoform has been associated with poor prognosis and chemoresistance in a wide array of cancers, including acute promyelocytic leukemia, breast, cervical, ovarian, and lung cancers (16–20). ΔNp73 possesses oncogenic properties that include impairment of the DNA damage-response pathway and cellular immortalization (21, 22). Moreover, it has dominant negative characteristics that inhibit p53 and TAp73 functions and promote cancer stemness, epithelial mesenchymal transition, hypoxia responses, angiogenesis, invasion and metastasis, and drug resistance, thus supporting carcinogenesis (23–28). In contrast to ΔNp73, TAp73 functions as a tumor suppressor similar to p53. It was shown to play a role in migration, invasion, apoptotic cell death, and macrophage-mediated innate immunity (29–33). TAp73 knockout (KO) mice spontaneously develop tumors, mainly lung adenocarcinoma, and TAp73 KO tumors have increased intratumoral vascularization (27, 32, 34).

To date, little is known about how TAp73 affects immune cell infiltration in the TME. Here, we report that low levels of TAp73

Significance

Breast cancer is one of the most prevalent cancers worldwide. Understanding this complex disease is therefore of great importance. Here, we report that loss of TAp73, a known tumor suppressor and member of the p53 protein family, leads to increased activation of the NF-κB pathway, secretion of the chemokine CCL2, and an increase in protumoral macrophage infiltration in human breast cancer. Both high levels of CCL2 and high macrophage infiltration are known to correlate with poor prognosis in breast cancer patients. This study identifies TAp73 as a regulator of macrophage recruitment and highlights a role for TAp73 in immune cell regulation in cancer.

Author contributions: J.W., H.A.M.S., L.Z., C.R., and M.T.W. designed research; J.W., H.A.M.S., L.Z., N.v.B., E.B., S.d.S.F., V.Z., M.S., C.R., and M.T.W. performed research; J.W., J.H., and M.T.W. contributed new reagents/analytic tools; J.W., H.A.M.S., L.Z., N.v.B., E.B., S.d.S.F., M.S., N.F., C.R., and M.T.W. analyzed data; and J.W. and M.T.W. wrote the paper.

The authors declare no competing interest.

This article is a PNAS Direct Submission.

[1]To whom correspondence may be addressed. Email: margareta.wilhelm@ki.se.

This article contains supporting information online at https://www.pnas.org/lookup/suppl/doi:10.1073/pnas.2017089118/-/DCSupplemental.

Published March 1, 2021.

in breast cancer strongly correlate with inflammation, immune cell infiltration, and an increased activation of the NF-κB pathway. Furthermore, we show that this increase in NF-κB activity enhances secretion of chemokines that promote chemotaxis and an increased influx of tumor-promoting macrophages that fuels tumor progression.

Results

Low TAp73 Expression Correlates with Increased Inflammation and Activation of the NF-κB Pathway in Breast Cancer Patients. TAp73 and ΔNp73 have been reported to have both opposing and overlapping functions in tumor development (35). To investigate specifically the role of TAp73 in breast cancer, we used the publicly available TCGA breast cancer data set (36), excluded all samples that expressed ΔNp73, and focused only on the ΔNp73-nonexpressing patient samples (flowchart in Fig. 1*A*). These samples were divided into high and low TAp73-expressing groups and analyzed for differential gene expression (Fig. 1*B* and Dataset S1). As expected, the most significantly down-regulated gene in the TAp73 Low patient group was *TP73* (Fig. 1*C*). In total, 317 genes were found to be down-regulated, including *KRT1*, previously shown to inhibit breast cancer cell invasion (37), and several genes involved in regulating multiciliated cell differentiation (*FOXJ1*, *CDC20B*, and *DRC1*) (Fig. 1*C*), confirming previous reports on the important role TAp73 plays in regulating multiciliogenesis (38). In addition, 746 genes were significantly up-regulated in the TAp73 Low group compared to the TAp73 High group (Fig. 1*B*). Interestingly, the most significantly up-regulated are genes regulating steroidogenesis (*CYP19A1*, *AKR1B15*, and *CYP11A1*). *CYP19A1* encodes for the enzyme Aromatase that is involved in biosynthesis of estrogens (39) and has been reported to be inhibited by p53 (40), our finding that *CYP191A1* is up-regulated in TAp73 Low tumors may suggest that TAp73, like p53, represses *CYP191A1* expression.

Breast cancer can be divided into clinical subtypes based on immunohistochemistry (IHC) for hormone receptors (HR), estrogen (ER) and progesterone (PR), and human epidermal growth factor receptor 2 (HER2), classifying tumors into $HR^+/HER2^-$, $HR^+/HER2^+$, $HR^-/HER2^+$, and triple negative (TNBC [$ER^-/PR^-/HER2^-$]), with TNBC and $HR^-/HER2^+$ considered the more aggressive subtypes with high need for additional oncological therapy (36, 41, 42). Interestingly, we observed a significant increase of $HR^-/HER2^+$ and TNBC subtypes in TAp73 Low tumors compared to TAp73 High tumors (*SI Appendix*, Fig. S1 *A* and *B*). Mutations in the TP53 gene are frequent in both $HR^-/HER2^+$ and TNBC subtypes (36); we thus analyzed the distribution of p53 mutations within the TAp73 High and Low subgroups and found an overrepresentation of p53 mutations in the TAp73 Low group compared to TAp73 High (*SI Appendix*, Fig. S1*C*). To study if the difference in distribution of subtypes between TAp73 High and Low tumors was due to the increase of p53mut tumors in TAp73 Low group, we reanalyzed subtype distribution comparing p53wt/TAp73 High versus p53wt/TAp73 Low or p53mut/TAp73 High versus p53mut/TAp73 Low subgroups. Importantly, although we observe more TNBC and $HR^-/HER2^+$ subtype tumors in the p53 mutant group, we observe a significant increase in TNBC and $HR^-/HER2^+$ subtypes in the TAp73 Low group compared to the TAp73 High group in both the p53 wild-type (WT) and mut samples (*SI Appendix*, Fig. S1*D*), suggesting that loss of TAp73 correlates with the more aggressive TNBC and $HR^-/HER2^+$ subtypes and that p53 mutation in combination with TAp73 is even stronger correlated in TNBC and $HR^-/HER2^+$ subtypes.

To understand which biological pathways are altered depending on TAp73 expression, we performed gene set enrichment analysis (GSEA) using the GO, Hallmark, and Reactome gene sets and found 828 gene sets to be significantly changed between the TAp73 Low versus TAp73 High tumors (Dataset S2). Enriched gene sets in the TAp73 Low tumors included interleukin-signal transducer and activator of transcription proteins (STAT) signaling, NF-κB signaling, inflammatory responses, and monocyte chemotaxis (Fig. 1*D*). Next, a pathway enrichment analysis was performed using Cytoscape and EnrichmentMap that cluster closely related gene sets and show gene overlap between gene sets (43). We identified 64 enriched clusters (containing ≥3 genesets) that could be further grouped into 8 main clusters based on biological function (Fig. 1*E* and Dataset S3); 7 clusters were enriched in the TAp73 Low group, while 1 cluster containing gene sets related to cilium and microtubule assembly was enriched in TAp73 High expressing tumors, again confirming the importance of TAp73 in cilia regulation (38).

The majority of enriched gene sets in TAp73 Low tumors were associated with immune responses (Fig. 1*E*), and we identified clusters of gene sets linked to immune cell regulation, chemotaxis, cytokine and calcium response, antigen presentation, phagocytosis, and immune cell differentiation (Fig. 1 *E* and *F*), suggesting that loss of TAp73 results in an inflammatory tumor milieu that will affect immune cell infiltration and function.

Considering that the majority of immune responses are regulated by the NF-κB pathway and that several NF-κB–related gene sets were found up-regulated in TAp73 Low tumors (Fig. 1*G* and Dataset S2), we hypothesized that loss of TAp73 would affect NF-κB activity. However, since p53 gain-of-function mutants have been shown to enhance NF-κB–mediated responses (44), we reanalyzed the differential gene expression and GSEA comparing TAp73 Low versus TAp73 High tumors only within the p53 wt group or within the p53 mutant group and found that TAp73 Low tumors showed an enrichment in genes involved in inflammatory response and NF-κB activation regardless of p53 status (*SI Appendix*, Fig. S1*E* and Dataset S4), suggesting that loss of TAp73 will enhance NF-κB–mediated responses. To test this, a NF-κB luciferase reporter construct containing NF-κB binding sites (BSs) was transfected into $TAp73^{+/+}$ and $TAp73^{-/-}$ E1A/H-Ras^{V12} transformed mouse embryonic fibroblasts ($MEF^{E1A/Ras}$) and luciferase levels were measured as a readout for NF-κB activity. Significantly higher NF-κB activity was detected in $TAp73^{-/-}$ $MEF^{E1A/Ras}$ compared to $TAp73^{+/+}$ $MEF^{E1A/Ras}$ cells (Fig. 1*H*). Additionally, several known NF-κB target genes were found up-regulated in both the TAp73 Low tumors and in $TAp73^{-/-}$ $MEF^{E1A/Ras}$ (Fig. 1*I* and Dataset S1), altogether suggesting that low levels or loss of TAp73 results in activation of the NF-κB pathway.

Loss of TAp73 Leads to Increased CCL2 Levels. Next, we analyzed the release of NF-κB–regulated cytokines from $TAp73^{+/+}$ and $TAp73^{-/-}$ $MEF^{E1A/Ras}$ into the cell culture media using a cytokine profiler array. Surprisingly, out of 40 cytokines analyzed, only 7 were found to be secreted at a detectable level (Fig. 2*A*). Of note, although *Cxcl10* messenger RNA (mRNA) expression was found to be significantly up-regulated in $TAp73^{-/-}$ $MEF^{E1A/Ras}$ (Fig. 1*I*), the Cxcl10 protein secretion was significantly lower in $TAp73^{-/-}$ $MEF^{E1A/Ras}$ compared to $TAp73^{+/+}$ $MEF^{E1A/Ras}$ (Fig. 2*A*). Interestingly, of the cytokines analyzed, Ccl2 was among the most abundantly secreted cytokines with significantly increased levels in $TAp73^{-/-}$ $MEF^{E1A/Ras}$ (Fig. 2*A*). Ccl2 is known to play an important role as a chemoattractant for monocytes and has been linked to poor prognosis in breast cancer (13).

To further validate the effect on Ccl2, we first confirmed the increase in *Ccl2* mRNA and protein levels in two different $TAp73^{-/-}$ $MEF^{E1A/Ras}$ cell lines (*SI Appendix*, Fig. S2*A* and Fig. 2*B*). In addition, increased Ccl2 protein secretion in $TAp73^{-/-}$ $MEF^{E1A/Ras}$ compared to $TAp73^{+/+}$ $MEF^{E1A/Ras}$ was confirmed using enzyme-linked immunosorbent assay (ELISA) (Fig. 2*C*). To validate the effect of TAp73 on Ccl2 regulation in a disease-relevant model, we crossed $TAp73^{+/+}$ and $TAp73^{-/-}$ mice with the MMTV-PyMT breast cancer model, collected spontaneously developing mammary tumors, and isolated PyMT/$TAp73^{+/+}$ and PyMT/$TAp73^{-/-}$

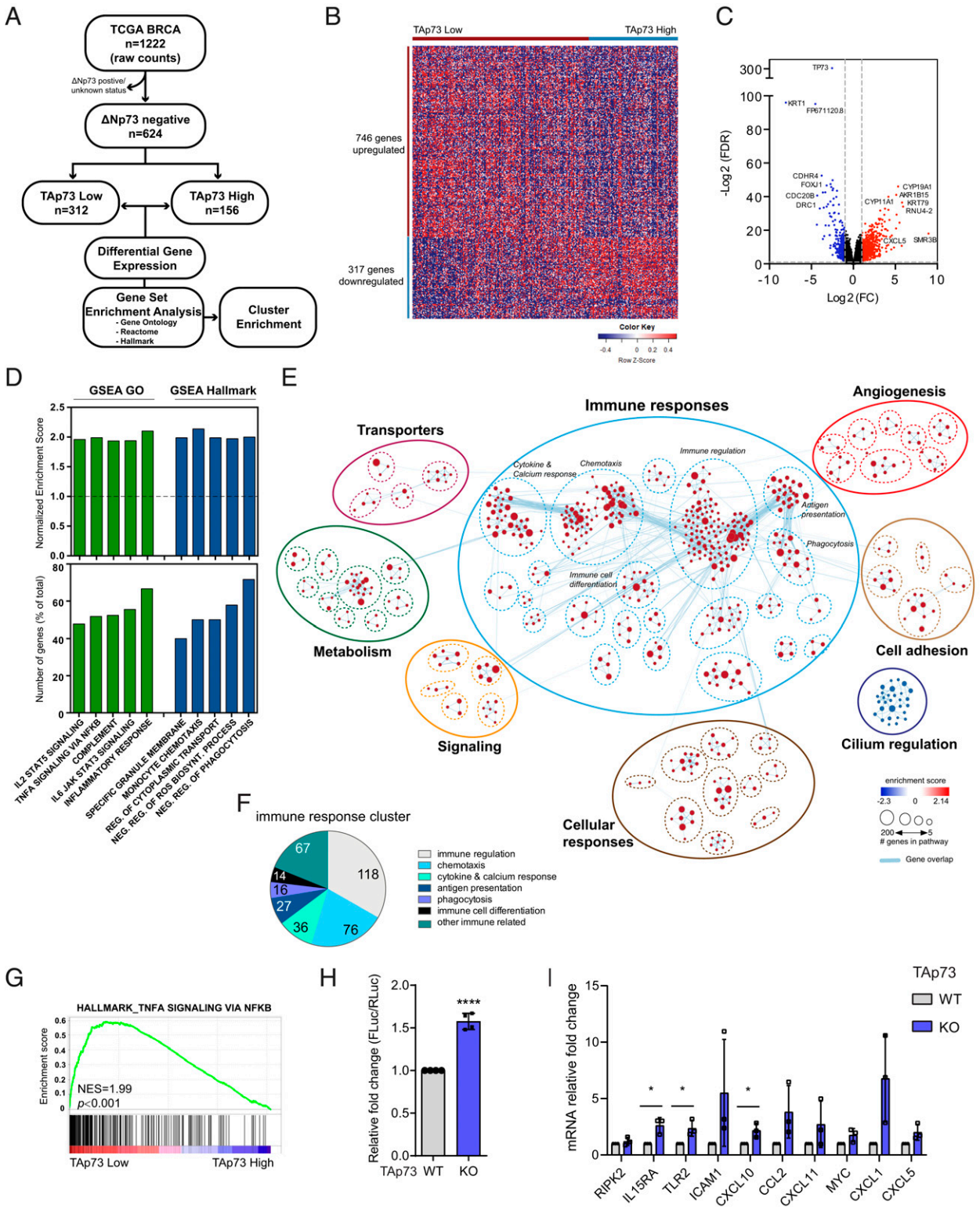

Fig. 1. Low levels of TAp73 correlate with an inflammatory signature and increased activity of the NF-κB pathway in breast cancer. (*A*) A flowchart of TCGA breast cancer data set analysis. (*B*) A heatmap based on differential gene set analysis comparing TAp73 low versus TAp73 high expressing samples (FC[Log2] >1, FDR > 0.05). (*C*) A volcano plot presenting differential gene expression as significance (FDR value) versus fold change. (*D*, *Top*) GO- and Hallmark-enriched gene sets in TAp73 Low tumors. (*E*) An enrichment map generated from GSEA results and visualized by Cytoscape EnrichmentMap and AutoAnnotate application, showing biological pathways enriched in TAp73 low versus TAp73 high. The red nodes represent up-regulated biological pathways, blue nodes represent down-regulated biological pathways, and blue lines represent gene overlap between pathways. (*F*) A cluster enrichment analysis within the immune response cluster showing number of significantly enriched gene sets/biological category. (*G*) An enrichment plot of a representative NF-κB gene set within the NF-κB gene set cluster. (*H*) NF-κB reporter assay was performed in TAp73 WT and KO MEF$^{E1A/Ras}$ (data shown as mean ± SD, $n = 3$, $P < 0.0001$). (*I*) qRT-PCR analysis of mRNA levels of selected NF-κB target genes comparing TAp73 KO to WT (data shown as mean ± SD, $n = 3$). *$P < 0.05$, ****$P < 0.0001$.

https://doi.org/10.1073/pnas.2017089118

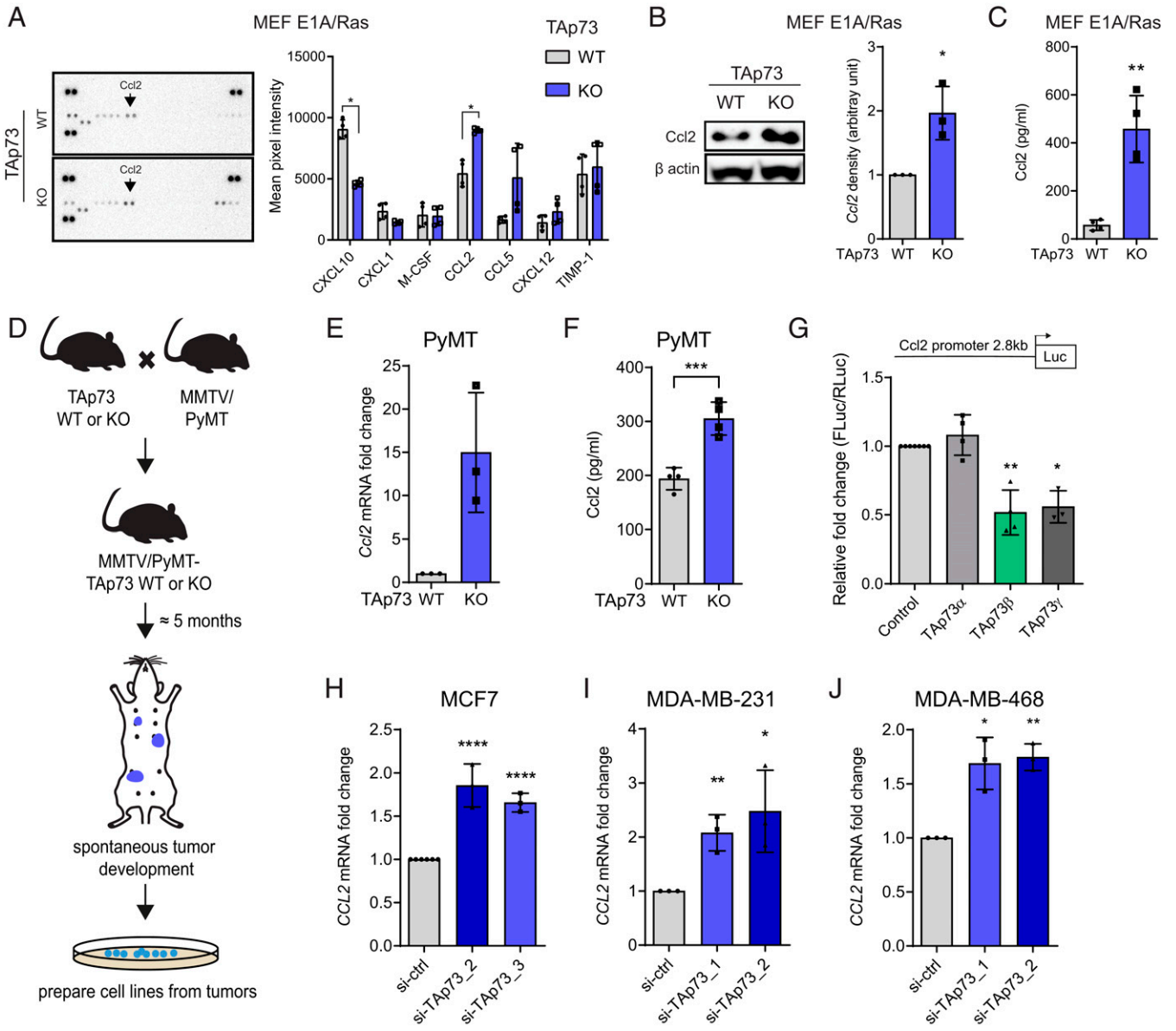

Fig. 2. TAp73 loss leads to increased Ccl2 expression in breast cancer cell lines. (*A*, *Left*) Representative cytokine profiler array analyzing cytokine content in conditioned media from TAp73 WT or KO MEF$^{E1A/Ras}$. (*Right*) Quantification of mean pixel intensity of all detected cytokines. (*B*) Representative Western blot showing Ccl2 protein levels in TAp73 WT and KO MEF$^{E1A/Ras}$, with Ccl2 protein quantification normalized to β-actin ($n = 3$). (*C*) ELISA analysis of Ccl2 protein secretion in conditioned media from TAp73 WT and KO MEF$^{E1A/Ras}$ ($n = 4$). (*D*) A schematic of how PyMT/TAp73 WT and KO cell lines were generated. (*E*) qRT-PCR analysis of Ccl2 mRNA levels in PyMT/TAp73 WT and KO cells ($n = 3$). (*F*) ELISA analysis of Ccl2 protein secretion in conditioned media from PyMT/TAp73 WT and KO cells ($n = 4$). (*G*) Ccl2 promoter luciferase reporter was cotransfected with different TAp73 isoforms in HEK293 cells. Luciferase activity was measured 24 h after transfection and normalized to mock control ($n = 4$). qRT-PCR analysis of *CCL2* mRNA expression after knockdown of TAp73 using two different siRNAs against TAp73 in (*H*) MCF7 ($n = 3$), (*I*) MDA-MB-231 ($n = 3$), and (*J*) MDA-MB-468 ($n = 3$). All data are shown as mean ± SD $^*P < 0.05$, $^{**}P < 0.01$, $^{***}P < 0.001$, $^{****}P < 0.0001$.

tumors cells (Fig. 2*D*). Importantly, we confirmed that PyMT/TAp73$^{-/-}$ cells express higher levels of *Ccl2* mRNA and secrete more Ccl2 protein compared to PyMT/TAp73$^{+/+}$ cells (Fig. 2 *E* and *F*).

Next, we reintroduced TAp73α, TAp73β, or TAp73γ in TAp73$^{-/-}$ MEF$^{E1A/Ras}$ and found that TAp73β and TAp73γ but not TAp73α down-regulates *Ccl2* mRNA levels (*SI Appendix*, Fig. S2 *B* and *C*). To further confirm the inhibitory effect of TAp73β and TAp73γ on Ccl2 expression, we coexpressed a Ccl2 reporter construct containing 2.8kb of the murine *Ccl2* promoter cloned upstream of a luciferase gene (45), with TAp73α, TAp73β, or TAp73γ and observed transcriptional repression of the *Ccl2* promoter by TAp73β and TAp73γ but not by TAp73α (Fig. 2*G*).

To substantiate our findings, we knocked down TAp73 using small interfering RNA (siRNA) in human breast cancer cell lines MCF7, MDA-MB-231, and MDA-MB-468. Knockdown of TAp73 resulted in an up-regulation of *CCL2* mRNA levels in all three cell lines (Fig. 2 *H–J* and *SI Appendix*, Fig. S2 *D–F*), while overexpression of TAp73β, but not TAp73α, led to a significant decrease in *CCL2* mRNA levels (*SI Appendix*, Fig. S2 *G–J*). The inhibitory effect of TAp73β on *Ccl2* expression was further validated in mouse breast cancer cell lines 4T1, E0771, and MMTV-PyMT (*SI Appendix*, Fig. S2 *K–N*). Taken together, our data demonstrate that TAp73 represses CCL2 expression, whereas KO or knockdown of TAp73 impedes this repression, resulting in increased CCL2 expression.

TAp73 Is Regulating Ccl2 Expression via Suppression of the NF-κB Pathway. Next, we investigated the mechanism by which TAp73 represses Ccl2 expression. Considering previous reports that the NF-κB pathway is one of the main regulators of Ccl2 (46) and our observation that NF-κB activity increases upon TAp73 loss, we inhibited this pathway with the IKKβ inhibitor SC-514 that blocks IkB phosphorylation and subsequent RelA/p65 nuclear translocation (*SI Appendix*, Fig. S3*A*). Treatment with the NF-κB inhibitor resulted in a concomitant decrease in *Ccl2* mRNA levels in both TAp73$^{+/+}$ and TAp73$^{-/-}$ MEF$^{E1A/Ras}$ (Fig. 3*A*) and TAp73$^{+/+}$ and TAp73$^{-/-}$ PyMT cells (Fig. 3*B*). Importantly, inhibition of the NF-κB pathway reverted Ccl2 protein secretion levels in TAp73$^{-/-}$ MEF$^{E1A/Ras}$ and TAp73$^{-/-}$ PyMT cells to protein levels observed in TAp73$^{+/+}$ cells (Fig. 3 *C* and *D*). Additionally, siRNA-mediated knockdown of RelA/p65 or treatment with a specific RelA/p65 inhibitor, JSH-23 (*SI Appendix*, Fig. S2*A*), resulted in a drastic decrease in Ccl2 mRNA levels and protein secretion (Fig. 3 *E–H* and *SI Appendix*, Fig. S3 *B–G*), suggesting that the increase in Ccl2 in TAp73$^{-/-}$ tumor cells is mediated by RelA/p65.

The Ccl2 promoter region contains four possible NF-κB response elements (Fig. 3*I*). The two most distal BSs (here called BS3 and BS4) have been shown to be important for RelA/p65-dependent Ccl2 regulation (45). To further confirm the role of TAp73 in inhibiting RelA/p65-mediated activation of the Ccl2 promoter, we deleted either BS3 or BS4 individually or together in the Ccl2 reporter construct and coexpressed it with TAp73β. Deletion of BS3 or BS4 resulted in a decrease of Ccl2 promoter activity; however, TAp73β was still able to further decrease it (Fig. 3*J*). In contrast, codeletion of BS3 and BS4 drastically reduced *Ccl2* promoter activity, and addition of TAp73β did not result in further reduction (Fig. 3*J*), demonstrating that BS3 and BS4 are required for *Ccl2* promoter activation and that TAp73β inhibits NF-κB–dependent transcriptional activation of the *Ccl2* promoter. Collectively, our data demonstrates that TAp73 is repressing the NF-κB pathway and that TAp73 loss results in NF-κB–mediated up-regulation of Ccl2.

Loss of TAp73 Leads to Increased Infiltration of Tumor-Promoting Macrophages in Experimental Mammary Tumor Models as well as Human Breast Cancer Patient Samples. CCL2 is one of the main chemokines regulating monocyte migration and has been shown to be crucial for attraction of TAMs in breast cancer (13). Interestingly, chemotaxis was one of the largest enriched gene set clusters in TAp73 Low breast cancer samples (Fig. 1*E*), and, in particular, we found that loss of TAp73 correlated with mononuclear cell migration as well as monocyte chemotaxis (Fig. 4 *A* and *B*). To study the effect TAp73 loss in tumor cells has on macrophage migration, we analyzed the migratory capacity of IC-21 mouse macrophages exposed to conditioned media from either TAp73$^{+/+}$ or TAp73$^{-/-}$ MEF$^{E1A/Ras}$ and TAp73$^{+/+}$ or TAp73$^{-/-}$ PyMT cells (Fig. 4*C*). Using a scratch assay, we observed a significant increase of macrophage migration when receiving conditioned media from TAp73$^{-/-}$ cells compared to TAp73$^{+/+}$ cells (Fig. 4 *D* and *E*), suggesting that loss of TAp73 in tumor cells will enhance secretion of chemokines promoting macrophage recruitment.

We have previously shown that TAp73 KO tumors have increased blood vessel formation and grow faster in nude mice (27). We analyzed sections of these tumors using the pan-macrophage marker F4/80 and found significantly more F4/80^{+} cells in sections from TAp73$^{-/-}$ tumors compared to TAp73$^{+/+}$ tumors (*SI Appendix*, Fig. S4*A*). To validate our findings in a disease-relevant and immunocompetent model, we injected PyMT/TAp73$^{+/+}$ or PyMT/ TAp73$^{-/-}$ cells orthotopically into the mammary fat pad of syngeneic WT C57BL/6 female mice, thus ensuring that only the tumor cells differ in TAp73 status, and all other cells are WT and not effected (Fig. 4*F*) and monitored for tumor growth. Interestingly, although we did not find any differences in proliferation rate in vitro (*SI Appendix*, Fig. S4*B*), we observed significantly faster tumor onset and growth of PyMT/TAp73$^{-/-}$ cells compared to PyMT/TAp73$^{+/+}$ cells in vivo (Fig. 4*G* and *SI Appendix*, Fig. S4*C*). Tumors were harvested and analyzed by flow cytometry at similar volume and weight (*SI Appendix*, Fig. S4 *D–F*) to allow for comparison of immune cell infiltration at the same stage of tumor development. Surprisingly, we could not observe any significant difference in total immune cell infiltration (CD45^{+}) into PyMT/TAp73$^{-/-}$ tumors (Fig. 4*H*); however, out of the CD45^{+} immune cells, there was a significantly higher percentage of macrophages (CD45^{+}/CD11b^{+}/Ly6G^{-}/F4/80^{+}) in PyMT/TAp73$^{-/-}$ tumors compared to PyMT/TAp73$^{+/+}$ tumors (Fig. 4*I*), demonstrating that loss of TAp73 leads to increased macrophage migration and infiltration into the TME.

Macrophage infiltration has been correlated with poor prognosis and advanced disease stage in many types of cancer (47, 48). However, macrophages can play dual roles by either inhibiting or supporting tumor development depending on their phenotype (49). Flow cytometry analysis showed increased surface expression of scavenger receptor A (CD204) and mannose receptor (CD206) on macrophages in PyMT/TAp73$^{-/-}$ tumors (Fig. 4 *J* and *K*). Both markers are commonly used to define a protumoral macrophage phenotype. In contrast, there was no significant change in markers associated with an anti-tumoral macrophage phenotype, including CD80, CD86 and MHC II (Fig. 4*L*). Similarly, we observed increased levels of CD206^{+} macrophages in TAp73$^{-/-}$ tumors derived from transformed MEF$^{E1A/Ras}$ (*SI Appendix*, Fig. S5 *A* and *B*). These tumors were also found to have increased mRNA levels of the protumoral macrophage markers *Mrc1* (CD206) and Arginase 1, while expression of the anti-tumoral marker *Nos2* (iNOS) remained unchanged (*SI Appendix*, Fig. S5*C*). Altogether showing that loss of TAp73 leads to increased infiltration of tumor-promoting macrophages.

Next, we again used the TCGA breast cancer data set to study if TAp73 status would correlate with macrophage infiltration in human breast cancer. Indeed, we found a negative correlation between *TP73* expression and the human panmacrophage marker CD68, as well as markers for tumor-promoting macrophages, CD163, CD206, and CCL8 (Fig. 5 *A–D*). To further validate our findings, we analyzed a cohort of human breast cancer tumor sections with IHC for CD68 or CD163 and correlated it with *TAp73* mRNA expression. In agreement with our previous data, we found that low levels of *TAp73* mRNA expression correlated with increased infiltration of CD68^{+} and CD163^{+} macrophages (Fig. 5 *E–G*). Interestingly, CD68^{+} and CD163^{+} macrophage infiltration increased with increasing tumor grade and in TNBC (Fig. 5 *H* and *I*). In addition, we observed a concomitated down-regulation of TAp73 expression with increasing tumor grade, albeit not statistically significant (Fig. 5*J*). In conclusion, our data shows that loss of TAp73 activates the NF-κB pathway and the release of chemokines that change the intratumoral milieu favoring increased infiltration of tumor-promoting macrophages (Fig. 5*K*).

Discussion

The composition of the TME plays an important role in determining tumor growth or repression. Especially the composition of recruited immune cells and their activation status affects tumor progression among which TAMs are often most abundant (50). The presence of TAMs correlates with poor prognosis in the majority of solid tumors (6). TAMs can promote tumor initiation and dissemination and have been shown to play a direct role regulating the angiogenic switch (9). Importantly, TAMs can suppress responses to treatment, including chemotherapy, irradiation, and targeted therapy (51). TAMs are a diverse

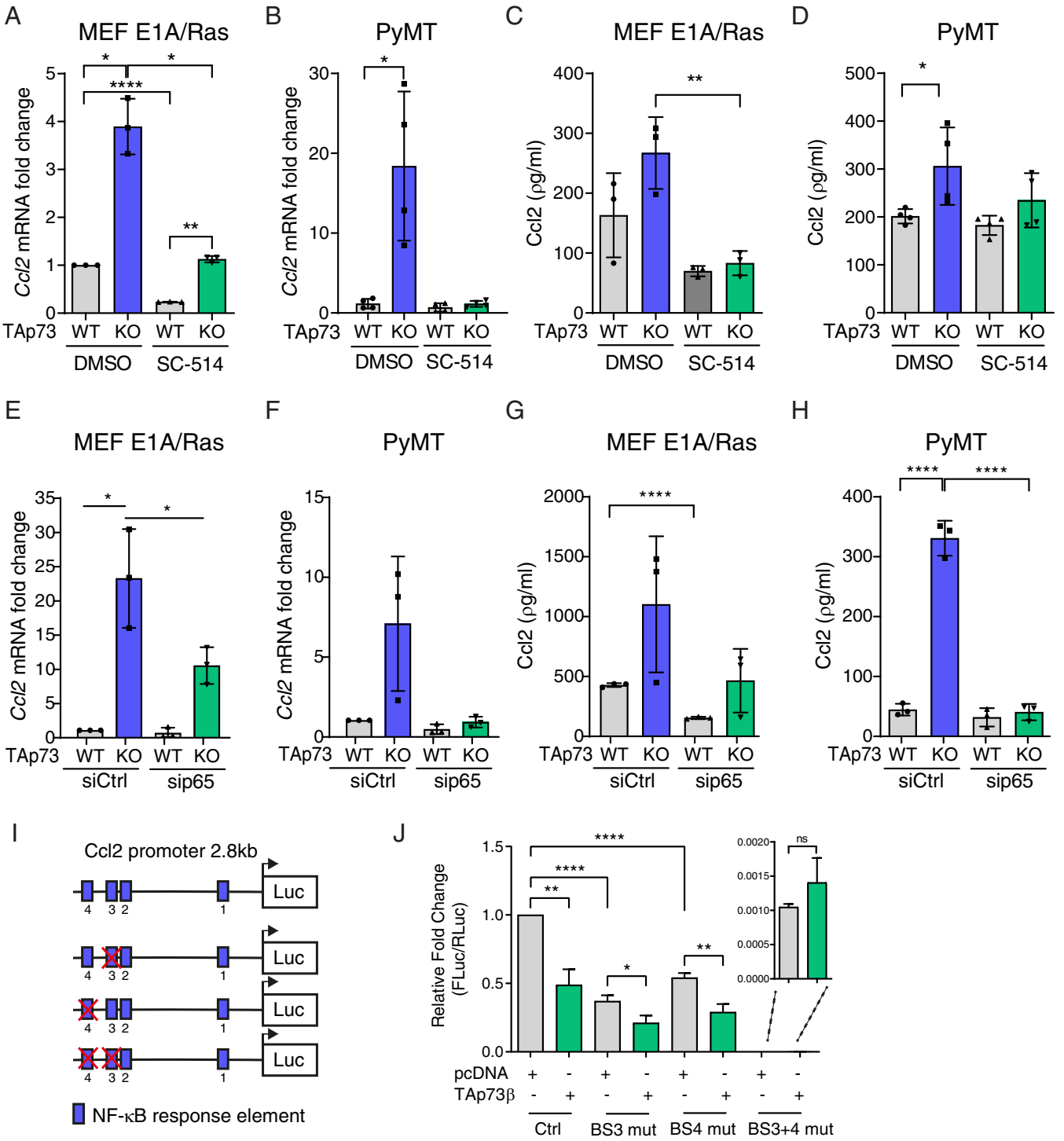

Fig. 3. TAp73 represses NF-κB–mediated regulation of Ccl2 expression. (*A*) qRT-PCR analysis of *Ccl2* mRNA levels in (*A*) TAp73 WT and KO MEF$^{E1A/Ras}$ ($n = 3$) and (*B*) PyMT/TAp73 WT or KO cells ($n = 4$) after 16-h treatment with NF-κB inhibitor SC-514 (100 μg/mL). ELISA analysis of Ccl2 protein secretion in conditioned media from (*C*) TAp73 WT and KO MEF$^{E1A/Ras}$ ($n = 3$) and (*D*) PyMT/TAp73 WT or KO cells ($n = 4$) after 16-h treatment with SC-514 (100 μg/mL). (*E* and *F*) qRT-PCR analysis of *Ccl2* mRNA levels in (*E*) TAp73 WT and KO MEF$^{E1A/Ras}$ ($n = 3$) and (*F*) PyMT/TAp73 WT or KO cells ($n = 3$) after 48-h treatment with sip65/RELA. (*G* and *H*) ELISA analysis of Ccl2 protein secretion in conditioned media from (*G*) TAp73 WT and KO MEF$^{E1A/Ras}$ ($n = 3$) and (*H*) PyMT/TAp73 WT or KO cells ($n = 3$) after 48-h treatment with sip65/RELA. (*I*) Schematics showing the murine Ccl2 promoter including NF-κB response elements, of which the distal BSs 3 and 4 were deleted either individually or simultaneously. (*J*) WT or mutated Ccl2 promoter luciferase reporter was cotransfected with TAp73β in HEK293 cells. Luciferase activity was measured 24 h after transfection and normalized to mock control ($n = 6$). All data are shown as mean ± SD *$P < 0.05$, **$P < 0.01$, ****$P < 0.0001$.

population of cells, classically divided into proinflammatory (M1, antitumoral) or anti-inflammatory (M2, protumoral) activity. However, transcriptome analyses have shown that TAMs cannot be categorized into distinct categories but display a wide range of biological activities based on developmental origin, tissue type, and surrounding environment (52, 53). TAMs are recruited into tumors by the chemokine CCL2 secreted from tumor cells. High CCL2 levels have been linked to increased metastasis in a number

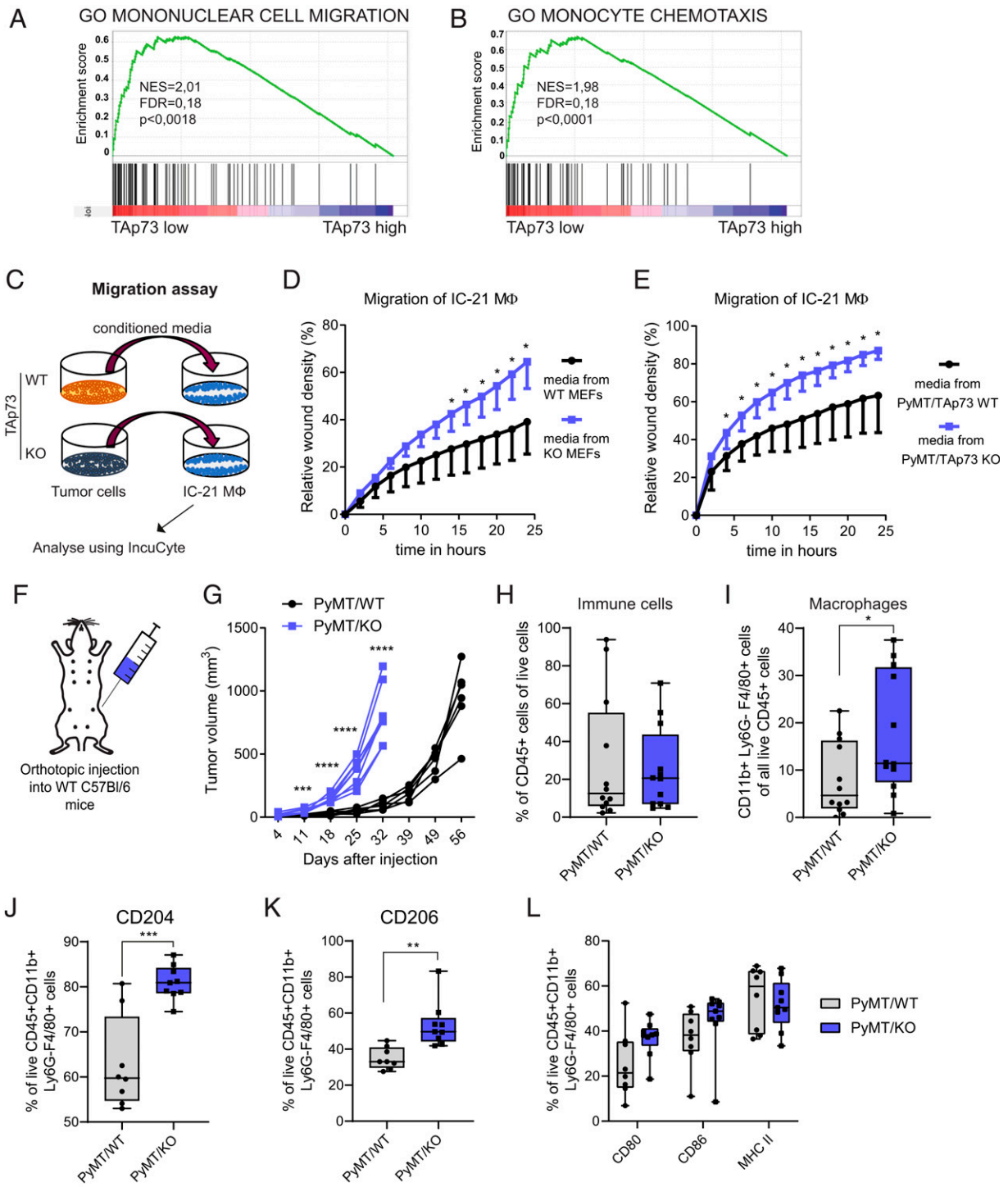

Fig. 4. TAp73 loss leads to increased macrophage migration and infiltration into mouse mammary tumors. Enrichment plots from GSEA showing significant enrichment of (*A*) "mononuclear cell migration" and (*B*) "monocyte chemotaxis" in TAp73 Low breast cancer tumors. (*C*) A schematic showing migration assay setup. A scratch was performed on IC-21 macrophages, which were exposed to conditioned media from TAp73 WT or KO tumor cells. IC-21 migration was quantified in real time using the IncuCyte system. (*D* and *E*) Quantification of IC-21 macrophage migration of a representative of the scratch assay over time after treatment with conditioned media of (*D*) TAp73 WT and KO MEF$^{E1A/Ras}$ ($n = 8$) and (*E*) PyMT/TAp73 WT or KO cells ($n = 5$ to 6). (*F*) A schematic of the orthotopic injection of PyMT/TAp73 cells into WT mice used for assessing TAM infiltration in immunocompetent mice. (*G*) Tumor growth over time of PyMT/TAp73 WT and KO tumors after orthotopic injection of 6×10^6 cells (presented as tumor volume; $n = 6$ to 8; $P > 0.0001$, two-way ANOVA, with multiple comparisons). (*H*) Flow cytometric analysis showing percentage of immune cells in PyMT/TAp73 WT and KO tumors, defined as live CD45$^+$ cells ($n = 12$). (*I*) Flow cytometric analysis showing percentage of macrophages in PyMT/TAp73 WT and KO tumors, defined as live CD45$^+$/CD11b$^+$/Ly6G$^-$/F4/80$^+$ cells ($n = 12$). A detailed gating strategy can be found in *SI Appendix*, Fig. S4*F*. (*J*, *K*) Flow cytometric analysis showing percentage of CD204$^+$ and CD206$^+$ macrophages, respectively, in PyMT/TAp73 WT and KO tumors, defined as live CD45$^+$/CD11b$^+$/Ly6G$^-$/F4/80$^+$ cells ($n = 8$ to 9). (*L*) Flow cytometric analysis showing percentage of CD80$^+$, CD86$^+$, or MHC II$^+$ macrophages in PyMT/TAp73 WT and KO tumors, defined as live CD45$^+$/CD11b$^+$/Ly6G$^-$/F4/80$^+$ cells ($n = 8$ to 9). *$P < 0.05$, **$P < 0.01$, ***$P < 0.001$, ****$P < 0.0001$.

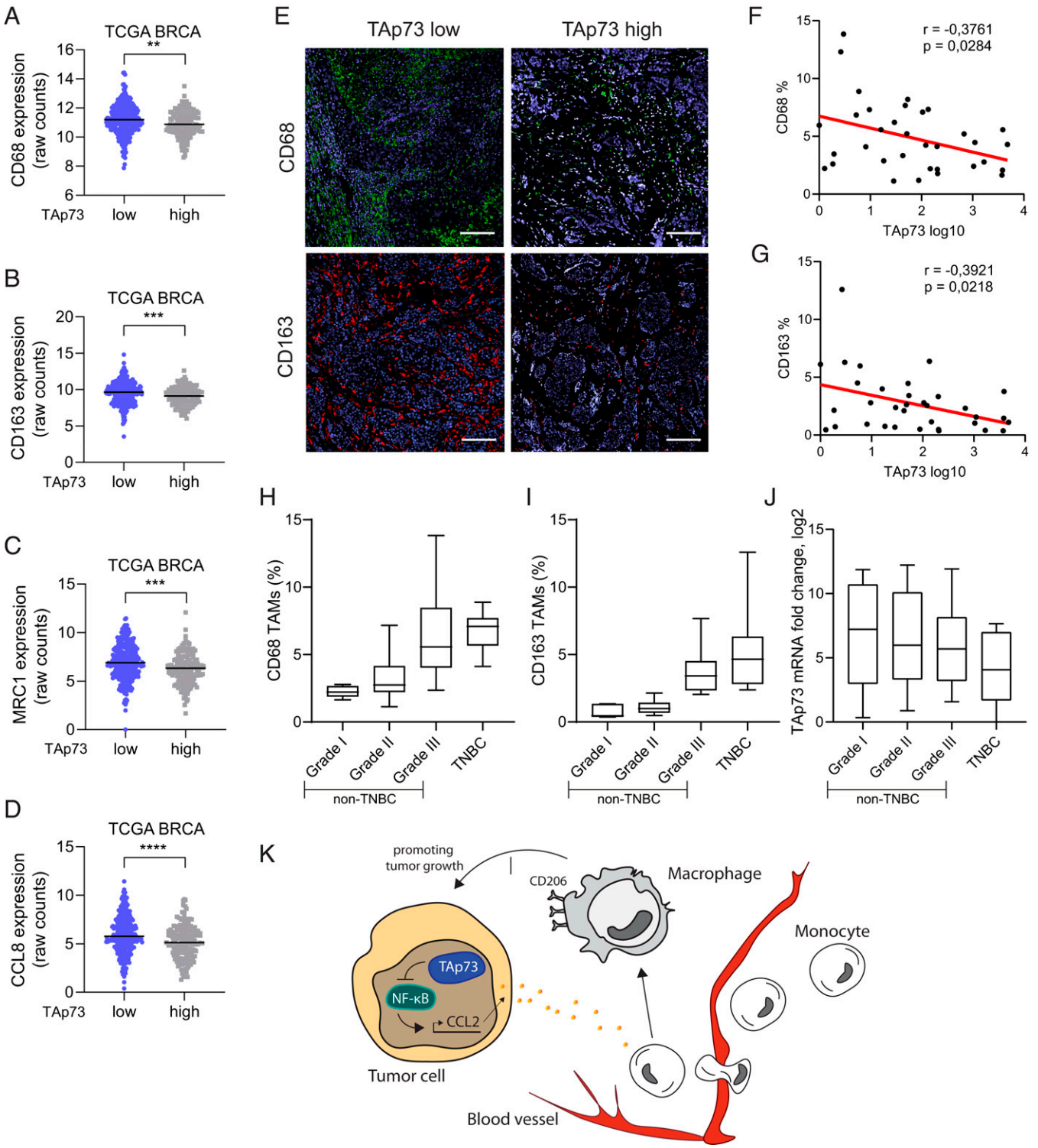

Fig. 5. TAp73 expression levels negatively correlate with macrophage markers in breast cancer patient biopsies. (*A–D*) Expression of CD68, CD163, MRC1 (CD206), or CCL8, respectively, in TAp73 High versus TAp73 Low TCGA breast cancer samples. (*E*) Representative immunofluorescence staining for macrophage markers CD68 (green) and CD163 (red) of breast cancer patient samples defined by low or high TAp73 expression; DAPI is shown in blue. (Scale bar, 100 μm.) (*F*, *G*) Correlation analysis between TAp73 expression levels and CD163+ or CD68+ macrophages, respectively ($n = 34$). (*H*) Percentage of CD68+ macrophages grouped by tumor grade ($n = 40$; $P > 0.0001$, one-way ANOVA). (*I*) Percentage of CD163+ macrophages grouped by tumor grade ($n = 40$; $P > 0.0001$, one-way ANOVA). (*J*) mRNA expression of TAp73 grouped by tumor grade ($n = 34$). (*K*) A schematic model of how TAp73 regulates CCL2 and concurrently results in macrophage infiltration into tumors. $^{*}P < 0.05$, $^{**}P < 0.01$, $^{***}P < 0.001$, $^{****}P < 0.0001$.

of cancers, including esophageal squamous-cell carcinoma, breast, colon, prostate, and lung cancers (54, 55). In addition to its role in monocyte and macrophage recruitment, CCL2 has been shown to contribute to a tumor-promoting phenotype of the recruited macrophages (56, 57) and to up-regulate CD206 on macrophages and rendering them more protumorigenic (58). The fact that CCL2 correlates with enhanced macrophage infiltration and poor patient survival suggests CCL2 as a promising target for cancer therapy. Inhibition of CCL2-CCR2 signaling in preclinical models has been shown to reduce TAM infiltration in both primary and metastatic lesions and to enhance the efficacy of therapy (13, 59–63). However, CCL2 blockage was reported to retain monocytes in the bone marrow, and ceasing the treatment resulted in massive macrophage infiltration into the TME and increased metastasis (64). Therefore, CCL2 blockage might not be a feasible treatment strategy, at least as single agent, without taking care of the excessive monocyte accumulation in the bone marrow.

We show here that TAp73 loss leads to increased expression of CCL2 and enhanced infiltration of macrophages in both mouse models and in breast cancer patients. In addition, we show that the macrophages in TAp73$^{-/-}$ tumors express higher levels of scavenger receptor A (CD204) and mannose receptor (CD206). These two receptors are commonly used to define a subset of tumor-promoting macrophages and are linked to worse prognosis in cancer patients (65, 66), demonstrating that loss of TAp73 changes the intratumoral milieu favoring infiltration tumor-promoting TAMs.

Interestingly, using TCGA data, we found that loss of TAp73 results in a global up-regulation of genes involved in immune responses and inflammation in breast cancer patients. This agrees with previous reports that complete loss of the *Trp73* gene in mice results in premature death due to chronic infections and inflammation (67). Furthermore, TAp73$^{-/-}$ mice have been shown to be more susceptible to septic shock due to impaired resolution of inflammatory responses and elevated production of TNFα and IL-6 in TAp73$^{-/-}$ macrophages (33). We identified NF-κB signaling as a possible mechanism for the up-regulation of immune-related genes and specifically for the up-regulation of Ccl2 in TAp73-deficient tumor cells, and inhibition of the NF-κB pathway and RelA/p65 normalized Ccl2 expression in TAp73$^{-/-}$ cells. Furthermore, deletion of NF-κB binding sites in the *Ccl2* promoter relieved the TAp73-mediated repression of *Ccl2* promoter activity, suggesting that TAp73 is blocking NF-κB–mediated promoter activity.

Intriguingly, reintroduction of TAp73β or TAp73γ, but not the TAp73α isoform, repressed *Ccl2* promoter activity and mRNA expression. In contrast to TAp73β and TAp73γ, TAp73α contains a sterile alpha motif (SAM) domain in the C-terminal part of the protein, which is thought to reduce transcriptional activity of TAp73α (15), that could explain why TAp73β and TAp73γ and not TAp73α showed an effect on Ccl2 regulation. In addition, TAp73β but not TAp73α has been shown to compete with RelA/p65 for binding to the transcriptional coactivator p300 (68). Loss of TAp73 would therefore lead to increased binding of RelA/p65 to p300 and induce transcription of NF-κB target genes, including chemokines such as CCL2. Similarly, p53 has also been found to compete with RelA/p65 for binding to p300 (69). Interestingly, mutant p53 was recently shown to promote inflammation and infiltration of microglia into glioblastoma via increased activation of the NF-κB pathway and concomitant CCL2 expression (70). Furthermore, ΔNp63, another member of the p53 family, was found to induce NF-κB–mediated expression of inflammatory genes in head and neck squamous cell carcinoma (71). Together with our findings, this suggests a crucial function for members of the p53 network in regulating NF-κB–mediated inflammation and immune cell infiltration in cancer.

In conclusion, we demonstrate that TAp73 regulates TAM infiltration through repression of NF-κB–mediated up-regulation of Ccl2. Our findings help to unravel the complexity of the p73 network and give insights into how TAp73 affects the immune cell compartment in breast cancer.

Materials and Methods

All animal experiments were conducted in accordance with guidelines of Karolinska Institutet and approved by Stockholm's North Ethical Committee of Animal Research. Breast cancer whole-tumor samples collection and analysis was approved by the Stockholm regional ethical committee (2016-957-31); patients with primary breast cancer in Stockholm were informed and offered to sign written informed consent regarding biobanking and research by their treating physician or research nurse. Detailed information about experimental design, including cell culture conditions, orthotopic injections, mRNA and protein expression assays, oligonucleotide sequences, antibodies, bioinformatic analyses, and statistical methods, can be found in *SI Appendix*.

Data Availability. All study data are included in the article and/or supporting information.

ACKNOWLEDGMENTS. We thank Professor Randall Johnson and Dr. Helene Rundqvist for providing MMTV-PyMT mice; Professor Mikael Karlsson and Dr. Saikieran Sedimbi for reagents, technical assistance, and helpful discussions; Janina Henze, Trixy Fang, Larsen Vornholz, and Robert Hanes for technical assistance; and Professor Marie Arsenian Henriksson and her laboratory for helpful discussions. This work was supported by grants from the Swedish Cancer Society (CAN2016/823, CF19_0460Pj), Radiumhemmets Forskningsfonder (#194162), and the Swedish Research Council (2016/00753 to M.W. and 2018-02915 to C.R.). M.W. is supported by a Young Investigator Award from the Swedish Cancer Society (CAN2012/1330).

1. F. R. Greten, S. I. Grivennikov, Inflammation and cancer: Triggers, mechanisms, and consequences. *Immunity* **51**, 27–41 (2019).
2. F. R. Balkwill, A. Mantovani, Cancer-related inflammation: Common themes and therapeutic opportunities. *Semin. Cancer Biol.* **22**, 33–40 (2012).
3. A. E. Ryan *et al.*, Targeting colon cancer cell NF-κB promotes an anti-tumour M1-like macrophage phenotype and inhibits peritoneal metastasis. *Oncogene* **34**, 1563–1574 (2015).
4. Y. Xia, S. Shen, I. M. Verma, NF-κB, an active player in human cancers. *Cancer Immunol. Res.* **2**, 823–830 (2014).
5. M. A. Huber *et al.*, NF-kappaB is essential for epithelial-mesenchymal transition and metastasis in a model of breast cancer progression. *J. Clin. Invest.* **114**, 569–581 (2004).
6. D. G. DeNardo, B. Ruffell, Macrophages as regulators of tumour immunity and immunotherapy. *Nat. Rev. Immunol.* **19**, 369–382 (2019).
7. B. Ruffell, N. I. Affara, L. M. Coussens, Differential macrophage programming in the tumor microenvironment. *Trends Immunol.* **33**, 119–126 (2012).
8. N. Linde *et al.*, Macrophages orchestrate breast cancer early dissemination and metastasis. *Nat. Commun.* **9**, 21 (2018).
9. E. Y. Lin *et al.*, Macrophages regulate the angiogenic switch in a mouse model of breast cancer. *Cancer Res.* **66**, 11238–11246 (2006).
10. C. E. Lewis, J. W. Pollard, Distinct role of macrophages in different tumor microenvironments. *Cancer Res.* **66**, 605–612 (2006).
11. B. Z. Qian, J. W. Pollard, Macrophage diversity enhances tumor progression and metastasis. *Cell* **141**, 39–51 (2010).
12. T. Kitamura *et al.*, CCL2-induced chemokine cascade promotes breast cancer metastasis by enhancing retention of metastasis-associated macrophages. *J. Exp. Med.* **212**, 1043–1059 (2015).
13. B. Z. Qian *et al.*, CCL2 recruits inflammatory monocytes to facilitate breast-tumour metastasis. *Nature* **475**, 222–225 (2011).
14. A. Rufini *et al.*, p73 in Cancer. *Genes Cancer* **2**, 491–502 (2011).
15. P. Vikhreva, G. Melino, I. Amelio, p73 alternative splicing: Exploring a biological role for the C-terminal isoforms. *J. Mol. Biol.* **430**, 1829–1838 (2018).
16. T. H. Leung *et al.*, The interaction between C35 and ΔNp73 promotes chemoresistance in ovarian cancer cells. *Br. J. Cancer* **109**, 965–975 (2013).
17. S. S. Liu *et al.*, Expression of deltaNp73 and TAp73alpha independently associated with radiosensitivities and prognoses in cervical squamous cell carcinoma. *Clin. Cancer Res.* **12**, 3922–3927 (2006).
18. A. R. Lucena-Araujo *et al.*, High ΔNp73/TAp73 ratio is associated with poor prognosis in acute promyelocytic leukemia. *Blood* **126**, 2302–2306 (2015).
19. H. Uramoto *et al.*, Expression of deltaNp73 predicts poor prognosis in lung cancer. *Clin. Cancer Res.* **10**, 6905–6911 (2004).
20. A. I. Zaika *et al.*, DeltaNp73, a dominant-negative inhibitor of wild-type p53 and TAp73, is up-regulated in human tumors. *J. Exp. Med.* **196**, 765–780 (2002).
21. O. Petrenko, A. Zaika, U. M. Moll, deltaNp73 facilitates cell immortalization and cooperates with oncogenic Ras in cellular transformation in vivo. *Mol. Cell. Biol.* **23**, 5540–5555 (2003).
22. M. T. Wilhelm *et al.*, Isoform-specific p73 knockout mice reveal a novel role for delta Np73 in the DNA damage response pathway. *Genes Dev.* **24**, 549–560 (2010).

23. C. Meier, P. Hardtstock, S. Joost, V. Alla, B. M. Pützer, p73 and IGF1R regulate emergence of aggressive cancer stem-like features via miR-885-5p control. *Cancer Res.* **76**, 197–205 (2016).
24. B. M. Pützer, DNp73: Oncotarget in invasion and metastasis. *Oncotarget* **5**, 3–4 (2014).
25. H. A. M. Sakil *et al*., ΔNp73 regulates the expression of the multidrug-resistance genes ABCB1 and ABCB5 in breast cancer and melanoma cells–A short report. *Cell Oncol. (Dordr.)* **40**, 631–638 (2017).
26. M. Steder *et al*., DNp73 exerts function in metastasis initiation by disconnecting the inhibitory role of EPLIN on IGF1R-AKT/STAT3 signaling. *Cancer Cell* **24**, 512–527 (2013).
27. M. Stantic *et al*., TAp73 suppresses tumor angiogenesis through repression of proangiogenic cytokines and HIF-1α activity. *Proc. Natl. Acad. Sci. U.S.A.* **112**, 220–225 (2015).
28. M. Stantic, J. Wolfsberger, H. A. M. Sakil, M. T. Wilhelm, ΔNp73 enhances HIF-1α protein stability through repression of the ECV complex. *Oncogene* **37**, 3729–3739 (2018).
29. R. C. Castellino *et al*., Overexpressed TP73 induces apoptosis in medulloblastoma. *BMC Cancer* **7**, 127 (2007).
30. V. Petrova *et al*., TAp73 transcriptionally represses BNIP3 expression. *Cell Cycle* **14**, 2484–2493 (2015).
31. J. Rodhe, E. Kavanagh, B. Joseph, TAp73β-mediated suppression of cell migration requires p57Kip2 control of actin cytoskeleton dynamics. *Oncotarget* **4**, 289–297 (2013).
32. R. Tomasini *et al*., TAp73 knockout shows genomic instability with infertility and tumor suppressor functions. *Genes Dev.* **22**, 2677–2691 (2008).
33. R. Tomasini *et al*., TAp73 is required for macrophage-mediated innate immunity and the resolution of inflammatory responses. *Cell Death Differ.* **20**, 293–301 (2013).
34. I. Amelio *et al*., TAp73 opposes tumor angiogenesis by promoting hypoxia-inducible factor 1α degradation. *Proc. Natl. Acad. Sci. U.S.A.* **112**, 226–231 (2015).
35. D. Engelmann, C. Meier, V. Alla, B. M. Pützer, A balancing act: Orchestrating amino-truncated and full-length p73 variants as decisive factors in cancer progression. *Oncogene* **34**, 4287–4299 (2015).
36. Cancer Genome Atlas Network, Comprehensive molecular portraits of human breast tumours. *Nature* **490**, 61–70 (2012).
37. V. Blanckaert *et al*., Docosahexaenoic acid inhibits the invasion of MDA-MB-231 breast cancer cells through upregulation of cytokeratin-1. *Int. J. Oncol.* **46**, 2649–2655 (2015).
38. A. Nemajerova *et al*., TAp73 is a central transcriptional regulator of airway multiciliogenesis. *Genes Dev.* **30**, 1300–1312 (2016).
39. S. Q. To, K. C. Knower, V. Cheung, E. R. Simpson, C. D. Clyne, Transcriptional control of local estrogen formation by aromatase in the breast. *J. Steroid Biochem. Mol. Biol.* **145**, 179–186 (2015).
40. X. Wang *et al*.; Kathleen Cuningham Foundation Consortium for Research into Familial Breast Cancer, Prostaglandin E2 inhibits p53 in human breast adipose stromal cells: A novel mechanism for the regulation of aromatase in obesity and breast cancer. *Cancer Res.* **75**, 645–655 (2015).
41. J. Hugh *et al*., Breast cancer subtypes and response to docetaxel in node-positive breast cancer: Use of an immunohistochemical definition in the BCIRG 001 trial. *J. Clin. Oncol.* **27**, 1168–1176 (2009).
42. C. M. Perou *et al*., Molecular portraits of human breast tumours. *Nature* **406**, 747–752 (2000).
43. J. Reimand *et al*., Pathway enrichment analysis and visualization of omics data using g:Profiler, GSEA, Cytoscape and EnrichmentMap. *Nat. Protoc.* **14**, 482–517 (2019).
44. T. Cooks *et al*., Mutant p53 prolongs NF-κB activation and promotes chronic inflammation and inflammation-associated colorectal cancer. *Cancer Cell* **23**, 634–646 (2013).
45. E. Mora, A. Guglielmotti, G. Biondi, P. Sassone-Corsi, Bindarit: An anti-inflammatory small molecule that modulates the NFκB pathway. *Cell Cycle* **11**, 159–169 (2012).
46. A. Ueda *et al*., NF-kappa B and Sp1 regulate transcription of the human monocyte chemoattractant protein-1 gene. *J. Immunol.* **153**, 2052–2063 (1994).
47. H. Jeong, I. Hwang, S. H. Kang, H. C. Shin, S. Y. Kwon, Tumor-associated macrophages as potential prognostic biomarkers of invasive breast cancer. *J. Breast Cancer* **22**, 38–51 (2019).
48. L. Cao *et al*., M2 macrophage infiltration into tumor islets leads to poor prognosis in non-small-cell lung cancer. *Cancer Manag. Res.* **11**, 6125–6138 (2019).
49. R. Tamura, T. Tanaka, Y. Yamamoto, Y. Akasaki, H. Sasaki, Dual role of macrophage in tumor immunity. *Immunotherapy* **10**, 899–909 (2018).
50. J. Wang, D. Li, H. Cang, B. Guo, Crosstalk between cancer and immune cells: Role of tumor-associated macrophages in the tumor microenvironment. *Cancer Med.* **8**, 4709–4721 (2019).
51. M. Lopez-Yrigoyen, L. Cassetta, J. W. Pollard, Macrophage targeting in cancer. *Ann. N. Y. Acad. Sci.*, 10.1111/nyas.14377 (2020).
52. J. G. Quatromoni, E. Eruslanov, Tumor-associated macrophages: Function, phenotype, and link to prognosis in human lung cancer. *Am. J. Transl. Res.* **4**, 376–389 (2012).
53. L. Cassetta *et al*., Human tumor-associated macrophage and monocyte transcriptional landscapes reveal cancer-specific reprogramming, biomarkers, and therapeutic targets. *Cancer Cell* **35**, 588–602.e10 (2019).
54. J. L. Steiner, E. A. Murphy, Importance of chemokine (CC-motif) ligand 2 in breast cancer. *Int. J. Biol. Markers* **27**, e179–e185 (2012).
55. M. J. Wolf *et al*., Endothelial CCR2 signaling induced by colon carcinoma cells enables extravasation via the JAK2-Stat5 and p38MAPK pathway. *Cancer Cell* **22**, 91–105 (2012).
56. R. Xu *et al*., CCL2 promotes macrophages-associated chemoresistance via MCPIP1 dual catalytic activities in multiple myeloma. *Cell Death Dis.* **10**, 781 (2019).
57. E. Sierra-Filardi *et al*., CCL2 shapes macrophage polarization by GM-CSF and M-CSF: Identification of CCL2/CCR2-dependent gene expression profile. *J. Immunol.* **192**, 3858–3867 (2014).
58. H. Roca *et al*., CCL2 and interleukin-6 promote survival of human CD11b+ peripheral blood mononuclear cells and induce M2-type macrophage polarization. *J. Biol. Chem.* **284**, 34342–34354 (2009).
59. K. A. Connolly *et al*., Increasing the efficacy of radiotherapy by modulating the CCR2/CCR5 chemokine axes. *Oncotarget* **7**, 86522–86535 (2016).
60. D. E. Sanford *et al*., Inflammatory monocyte mobilization decreases patient survival in pancreatic cancer: A role for targeting the CCL2/CCR2 axis. *Clin. Cancer Res.* **19**, 3404–3415 (2013).
61. A. Kalbasi *et al*., Tumor-derived CCL2 mediates resistance to radiotherapy in pancreatic ductal adenocarcinoma. *Clin. Cancer Res.* **23**, 137–148 (2017).
62. Z. G. Fridlender *et al*., CCL2 blockade augments cancer immunotherapy. *Cancer Res.* **70**, 109–118 (2010).
63. T. M. Nywening *et al*., Targeting both tumour-associated $CXCR2^+$ neutrophils and $CCR2^+$ macrophages disrupts myeloid recruitment and improves chemotherapeutic responses in pancreatic ductal adenocarcinoma. *Gut* **67**, 1112–1123 (2018).
64. L. Bonapace *et al*., Cessation of CCL2 inhibition accelerates breast cancer metastasis by promoting angiogenesis. *Nature* **515**, 130–133 (2014).
65. Y. He *et al*., Clinical and transcriptional signatures of human CD204 reveal an applicable marker for the protumor phenotype of tumor-associated macrophages in breast cancer. *Aging (Albany NY)* **11**, 10883–10901 (2019).
66. P. Allavena *et al*., Engagement of the mannose receptor by tumoral mucins activates an immune suppressive phenotype in human tumor-associated macrophages. *Clin. Dev. Immunol.* **2010**, 547179 (2010).
67. A. Yang *et al*., p73-deficient mice have neurological, pheromonal and inflammatory defects but lack spontaneous tumours. *Nature* **404**, 99–103 (2000).
68. S. M. Ryou *et al*., Functional cross-talk between p73beta and NF-kappaB mediated by p300. *Biochem. Biophys. Res. Commun.* **345**, 623–630 (2006).
69. G. A. Webster, N. D. Perkins, Transcriptional cross talk between NF-kappaB and p53. *Mol. Cell. Biol.* **19**, 3485–3495 (1999).
70. S. W. Ham *et al*., TP53 gain-of-function mutation promotes inflammation in glioblastoma. *Cell Death Differ.* **26**, 409–425 (2019).
71. Yang *et al*., ΔNp63 versatilely regulates a broad NF-κB gene program and promotes squamous epithelial proliferation, migration and inflammation. *Cancer Res.*, 10.1158/0008-5472.CAN-10-3445 (2011).